

# A Deep Learning MI-EEG Classication Model for BCIs

**Dose, Hauke; Møller, Jakob Skadkær; Puthusserypady, Sadasivan; Iversen, Helle K.**

*Published in:*
Proceedings of 2018 26th European Signal Processing Conference

*Link to article, DOI:*
10.23919/EUSIPCO.2018.8553332

*Publication date:*
2018

*Document Version*
Peer reviewed version

# A Deep Learning MI-EEG Classification Model for BCIs

Hauke Dose*, Jakob S. Møller, and Sadasivan Puthusserypady
Department of Electrical Engineering
Technical University of Denmark
2800 Kongens Lyngby, Denmark
*Email: hauke.dose@rwth-aachen.de

Helle K. Iversen
Stroke Unit, Department of Neurology
Rigshospitalet, University of Copenhagen
2600 Glostrup, Denmark
Email: helle.klingenberg.iversen@regionh.dk

***Abstract*—Reliable signal classification is essential for using an electroencephalogram (EEG) based Brain-Computer Interface (BCI) in motor imagery (MI) training. While deep learning (DL) is used in many areas with great success, only a limited number of works investigate its potential in this domain. This study presents a DL approach, which could improve or replace current state-of-the-art methods. Here, an end-to-end convolutional neural network (CNN) model is presented, which can be applied to raw EEG signals. It consists of a temporal and spatial convolution layer for feature extraction and a fully connected (FC) layer for classification. The global models were trained on 3s segments of EEG data. Training a subject-independent global classifier reaches 80.10%, 69.72%, and 59.71% mean accuracy for a dataset with two, three, and four classes, respectively, validated in 5-fold crossvalidation. Retraining the global classifier with data from single individuals improves the overall mean accuracy to 86.13%, 79.05%, and 68.93%, respectively. The results are superior to the results reported in the literature on the same data. Generally, the reported accuracy values are comparable with related studies, which shows that the model delivers competitive results. As raw signals are used as input, no pre-processing is needed, which qualifies DL methods as a promising alternative to established EEG classification methods.**

## I. Introduction

Stroke is one of the leading causes of adult disability leaving a large part of those surviving the incident with some form of hemiparesis or hemiplegia, which brings a heavy burden to the patient, family and healthcare systems [1]. Conventional therapy focuses on physiotherapy and repetitive training for functional recovery. New therapy forms are using Brain-Computer Interface (BCI) systems have emerged to tackle the limitations of the current stroke rehabilitation methods.

BCIs were already successfully used to control electric wheelchairs [2], for text input [3], or to create neural bypasses to control paretic limbs [4]. In stroke rehabilitation, they can be used for motor imagery (MI) training. MI (i.e. imagining the execution of movements) activates similar brain pathways as actual movements do. It shows promise to act as substitute exercises in situations where there is no residual motor function, or to prevent exhaustion [5], [6].

The dominating approach for extracting features from MI-EEG signals is the common spatial pattern (CSP) algorithm [7], [8] and variations thereof like common spatio-spectral patterns (CSSP) [9], filter bank CSP (FBCSP) [10], [11], or strong uncorrelating transform complex CSP (SUTCCSP) [12], [13]. The features are then classified through supervised learning algorithms like support vector machines (SVMs). Specialized pre-processing like linear filtering, artifact removal, and trial rejection often needs to be applied in order to achieve acceptable results.

While deep learning (DL) is conquering many domains [14], only few attempts have been made to use DL methods for MI signal classification. Only recently Kumar et al. suggested replacing commonly used classifiers like SVMs by multilayer perceptrons (MLP) while keeping the specialized feature extraction mechanisms [15]. Bashivan et al. used CNNs to classify EEG signals through spectral topography maps generated from short-time Fourier transformed (STFT) recordings [16]. Finally, Tabar et al. used time-frequency maps from STFT as input to a CNN with stacked auto-encoders (SAE) reaching very high accuracy compared to benchmark methods [17].

The approaches applied in [15]–[17] involve pre-processing like feature extraction or STFT for time-frequency mapping. The authors of [18] proposed an end-to-end DL approach using CNNs and long short-term memory cells (LSTMs) to classify raw EEG data without any pre-processing applied. Schirrmeister et al. developed a model with CNN input stages for separated temporal and spatial filtering yielding exceptional results despite a very simple and shallow architecture [19]. In the following, we will present a similar architecture and apply it to the Physionet database [20] of MI recordings.

## II. Method

The applied classification model is based on the shallow CNN proposed in [19]. It consists of two 1-D convolutional layers with 40 filter kernels per layer. While the first layer applies convolution along the time axis, the second layer learns a spatial filter along the EEG channel dimension, which creates weighed linear combinations of the single channel values. That is, this layer reduces the dimensionality of the data along the EEG channel dimension to one. Thereafter temporal mean pooling is applied to reduce the length of the data further, before the signal is passed to a fully connected layer for classification. Table I lists all layers of the model and some of their properties.

ISBN 978-90-827970-1-5 

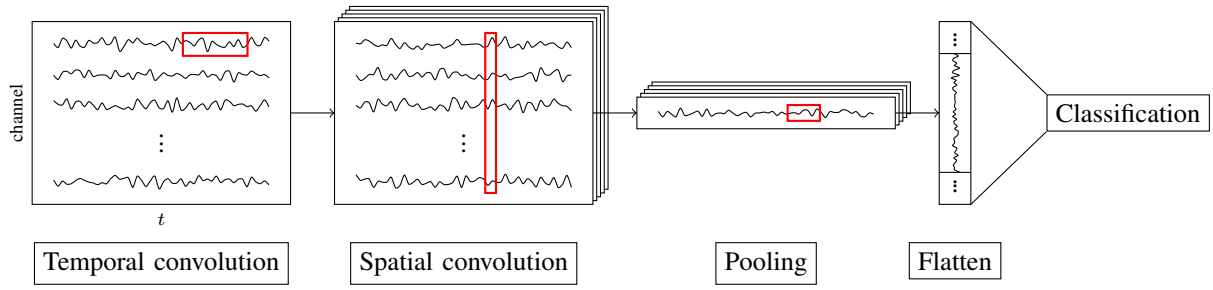


Fig. 1. Conceptual architecture of the CNN model. The two convolutional layers each perform a 1-D convolution on different axes. The rectangles (red) indicate the filter/pooling directions.

TABLE I
LISTING OF THE NEURAL NETWORK LAYERS: $N$ IS THE NUMBER OF SAMPLES PER INPUT SIGNAL AND $N_{\text{EEG}}$ IS THE NUMBER OF EEG CHANNELS USED. THE PARAMETER COUNTS ARE PROVIDED FOR TWO CLASS CLASSIFICATION OF 6S OF EEG DATA FROM $N_{\text{EEG}} = 64$ CHANNELS.

| type | kernel | padding | params | output shape |
|---|---|---|---|---|
| Conv 40 | $30 \times 1$ | same | 1240 | $N \times N_{\text{EEG}} \times 40$ |
| Conv 40 | $1 \times N_{\text{EEG}}$ | valid | 102440 | $N \times 1 \times 40$ |
| Avg. pool | $15 \times 1$ | valid | 0 | $\frac{N}{15} \times 1 \times 40$ |
| Flatten | - | - | 0 | $\frac{40N}{15}$ |
| FC 80 | - | - | 201680 | 80 |
| Softmax | - | - | 162 | 2 |
| | | | 305522 | |

To illustrate, Fig. 1 depicts the different processing steps on a higher level. The different layers are inspired by a typical signal processing pipeline. First, a filter bank of 40 FIR-filters pre-filters the signals of every EEG channel. It is reasonable to assume, that the model will learn filters that are used for frequency separation, to enable differentiation between significant frequency bands and to attenuate activity in insignificant frequency ranges. The subsequent spatial filters take into account the relation between EEG channels and likely learn filters that achieve a high inter-class variance to facilitate the classification through the FC/Softmax layers.

The model used the categorical cross-entropy loss-function and the Adam optimizer for batch training with a batch size of 16 trials. No further regularization was applied, as it did not show to improve the generalization performance. It was implemented[1] in a Python environment using the libraries tensorflow and keras on a consumer laptop with dedicated GPU, which was used for training and evaluation of the model. The training time of the model was typically less than 10 minutes per training/test data pair.

[1]The source code is available at https://github.com/hauke-d/cnn-eeg

## III. DATA

The model was applied to the Physionet EEG Motor Movement/MI Dataset [20], which was recorded by the developers of the BCI2000 system [21]. It was recorded in an EEG setup with 64 electrodes and the signals were sampled at 160 Hz. The data contains recordings of motor execution, as well as MI tasks. Only the MI trials are considered in this work. There are recordings from 109 different subjects performing two different MI tasks (left/right fist *or* both fists/both feet) in two-minute runs of each MI of the two tasks. One trial consists of 2 s rest, 4s of cued MI, and again 2s of rest before the next trial starts. Three subsets were created:

- **2-class (L/R)**: Distinction between left (L) and right (R) fist MI. Due to missing trials, a subset of 105 subjects and 42 trials per subject (21 for each side) were selected.
- **3-class (L/R/0)**: Random sections from the available baseline recordings (eyes opened) were included symbolizing the resting state (0). To uphold the class balance, the data was extended to 63 trials per subject.
- **4-class (L/R/0/F)**: Trials with the class "both feet" (F) from the second MI task were included as well resulting in 84 trials per subject.

For the model crossvalidation, the data was separated into five 80/20 splits by subject. This ensures that the test data is always from different subjects, than the model was trained on, which ensures that the results capture the generalization performance of the model. If not mentioned otherwise, the global average accuracy across all splits is reported in the result section.

## IV. RESULTS

In the following, we will present and analyze different aspects of the achieved classification performance and the learned model parameters.

### A. Global classifier

First, the performance of the global model was determined. When training and evaluating the model on full trials of 6s (including 1s of rest before and after the cue period), a crossvalidation accuracy of **87.98%**, **76.61%**, and **65.73%**,

ISBN 978-90-827970-1-5 © EURASIP 2018

TABLE II
CONFUSION MATRIX FOR 4 CLASS CLASSIFICATION. MANY L, R, AND F SAMPLES ARE CLASSIFIED AS 0 LEADING TO CLASS 0 FEATURING THE HIGHEST RECALL, BUT THE LOWEST PRECISION.

| | | predicted | | | | |
|---|---|---|---|---|---|---|
| | | L | R | 0 | F | recall |
| actual | L | 325 | 16 | 100 | 42 | 0.672 |
| | R | 15 | 287 | 120 | 61 | 0.594 |
| | 0 | 28 | 46 | 358 | 51 | 0.741 |
| | F | 39 | 16 | 96 | 332 | 0.687 |
| precision | | 0.799 | 0.786 | 0.531 | 0.683 | |

TABLE III
ACCURACY VALUES $p_0$ (GLOBAL CLASSIFIER) AND $\bar{p}_s$ (MEAN OF SUBJECT-SPECIFIC CLASSIFIERS) FOR A CLASSIFIER USING 64 CHANNELS AND 3S INPUT SEGMENTS.

| | $p_0$ | $\bar{p}_s$ | $\bar{p}_s$ - $p_0$ |
|---|---|---|---|
| 2 classes | 0.8010 | 0.8613 | +6.03% |
| 3 classes | 0.6972 | 0.7905 | +9.34% |
| 4 classes | 0.5971 | 0.6893 | +9.22% |

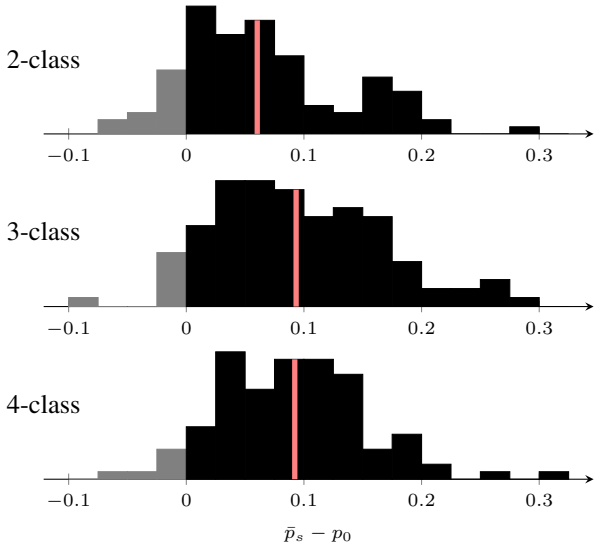


Fig. 2. Distribution of improvement in accuracy through subject-specific retraining. While improvements of up to 30 percentage points occur, only few subjects do not benefit from adapting the global modal on their data. The mean improvement is shown in red.

respectively for the two-, three-, and four-class classification task was reached. Reducing the amount of input data to the first three seconds after the MI cue delivered global accuracy values of **80.10%**, **69.72%**, and **59.71%**, respectively. The significantly lower performance is likely a result of additional information from the end of the MI period, which was no longer part of the input data.

Table II contains a typical confusion matrix for one test set from the 4-class task. Evidently, many samples are falsely classified as 0, leading to a low precision, but a high recall on the 0 class. This shows that the model tends to classify samples as 0 if it is uncertain. Intuitively, this makes sense, as trials with less distinctive MI features may look like the subject is resting and not performing any task at all.

### B. Subject-specific classifier

The analysis in the previous section suggests, that there may be subjects, which yield a lower individual accuracy, because they either feature less distinctive MI features or highly individual features, which differ from most of the other subjects such that the global model does not learn them well. Therefore, adapting the global classifier to a single subject can help increase the performance.

For this purpose, first the global model was trained as before. Then, for each subject in the associated test set, the training was continued on 75 % of the subject's data and evaluated on 25% of the data in a four-fold crossvalidation for five more epochs (passes through the training data). Table III compares the global average performance values before ($p_0$) and after ($\bar{p}_s$) adapting the model. For the two class set an improvement of around 6% was achieved, while for the remaining sets, the performance increase was more than 9%.

Fig. 2 shows the associated distribution of per-subject improvements through the subject-specific training. It reveals that improvements of up to 30 percentage points could be reached for single individuals, whereas it only had a negative impact for few subjects. This motivates the adaptation of the global model, if the effort of an initial calibration session to record subject-specific data can be tolerated.

### C. Learned spatial filters

As the model learns spatial filters like in CSP-related methods, it is possible to examine the learned weights and interpret them as individual filters for certain purposes. Some representative examples were chosen in Fig. 3. As one EEG channel's signal produces 40 differently filtered versions in the first layer of the model, the spatial filters shown have been averaged over this dimension to obtain a mean representation for all representations of the EEG signal. This naturally leads to averaging effects making the filters less distinct.

The top row contains filters that are assumed to react to actual MI activity. These filters are more sparse than found in other approaches (e.g. [7], [10], [12]), where filters often pronounce larger groups of adjacent electrodes. As the neural network model learns many filters, it likely obtains more fine-grained features as opposed to a few filters which simply maximize the global inter-class variance.

Finally, given that the model operates on raw EEG signals, it has to account for artifacts and unwanted signal components itself. The filters 32, 35 in Fig. 3 were found to resemble artifact filters for electromyography (EMG) components and filter 9 likely reacts to electrooculography (EOG) signals. This could be further examined by inspecting the single filter activation in response to certain characteristic input samples.

ISBN 978-90-827970-1-5 © EURASIP 2018

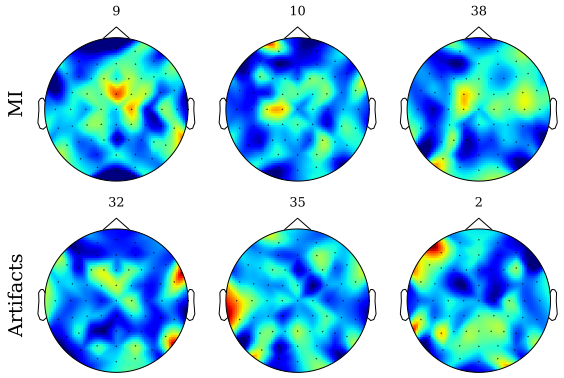


Fig. 3. Examples of the spatial filters of a three class classifier averaged over the feature dimension from the temporal filtering. While the upper filters are likely to respond to actual MI activity, the lower filters are assumed to react to artifacts like EMG and EOG activity.

TABLE IV
WORKS ON L/R CLASSIFICATION WITH THE PHYSIONET EEG DATASET.

| Work | $N_{\text{EEG}}$ | Training | Max. acc. | Methods |
|---|---|---|---|---|
| Park et al. [12] | 58 | global | 72.37% | SUT-CCSP SVM |
| Kim et al. [13] | 14 | subject | 80.05% | SUT-CCSP Random forest |
| This work | 64 | global | 80.10% | CNN |
| | | subject | 86.13% | |
| | 14 | global | 76.66% | CNN |
| | | subject | 82.66% | |

## V. DISCUSSION & CONCLUSION

We have presented a DL approach to classifying raw MI-EEG signals without domain-specific preprocessing like artifact rejection or band-pass filtering. Furthermore, the model can be adapted to single subjects increasing the individual classification performance by means of a short re-training session. The results for both the global and subject-specific classifier are competing with current state of the art methods.

To the best of our knowledge, the reached mean accuracy of **80.10 %** for a global two-class classifier and **86.13 %** for a subject-specific classifier is superior to all other works, which operate on the same underlying data. Table IV lists the two best approaches for global and subject-specific classifiers in comparison to the results achieved using the presented CNN model. Even when using the exact same selection of channels as in [13] for comparison, the achieved accuracy was increased by around 2.5 percentage points. Even with only 14 channels selected, the best known global classifier was beat by more than 3 percentage points, although it used far more electrodes.

These results have to be confirmed on different data, but they indicate that DL is a viable alternative to the current state-of-the art methods considering the mentioned advantages. Further research has to focus on the real-time applicability for online feedback to be able to employ the model in clinical practice.

## REFERENCES

[1] World Stroke Organization (WSO), "WSO background and mission statement," *Annual Report*, p. 6, 2016.
[2] F. Galán, M. Nuttin, E. Lew, P. Ferrez, G. Vanacker, J. Philips, and J. del R. Millán, "A brain-actuated wheelchair: Asynchronous and non-invasive brain–computer interfaces for continuous control of robots," *Clinical Neurophysiology*, vol. 119, no. 9, pp. 2159 – 2169, 2008.
[3] C. Guan, M. Thulasidas, and J. Wu, "High performance P300 speller for brain-computer interface," in *IEEE International Workshop on Biomedical Circuits and Systems, 2004.*, 12 2004.
[4] B. M. Young, J. Williams, and V. Prabhakaran, "BCI-FES: could a new rehabilitation device hold fresh promise for stroke patients?" *Expert Review of Medical Devices*, vol. 11, no. 6, pp. 537–539, 2014.
[5] M. Lotze and U. Halsband, "Motor imagery," *Journal of Physiology - Paris*, vol. 99, no. 4-6, pp. 386 – 395, 2006.
[6] T. Mulder, "Motor imagery and action observation: cognitive tools for rehabilitation," *Journal of Neural Transmission*, vol. 114, no. 10, pp. 1265–1278, 10 2007.
[7] Y. Wang, S. Gao, and X. Gao, "Common spatial pattern method for channel selection in motor imagery based bci," *2005 IEEE Engineering in Medicine and Biology 27th Annual Conference*, pp. 5392–5395, 2005.
[8] M. Grosse-Wentrup and M. Buss, "Multiclass common spatial patterns and information theoretic feature extraction," *IEEE Transactions on Biomedical Engineering*, vol. 55, no. 8, pp. 1991–2000, 8 2008.
[9] A. S. Aghaei, M. Mahanta, and K. Plataniotis, "Separable common spatio-spectral patterns for motor imagery BCI systems," *IEEE Transactions on Biomedical Engineering*, vol. 63, no. 1, pp. 15–29, 1 2016.
[10] K. K. Ang, Z. Y. Chin, H. Zhang, and C. Guan, "Filter bank common spatial pattern (FBCSP) in brain-computer interface," in *2008 IEEE International Joint Conference on Neural Networks (IEEE World Congress on Computational Intelligence)*, 6 2008, pp. 2390–2397.
[11] M. Bentlemsan, E. Zemouri, D. Bouchaffra, B. Yahya-Zoubir, and K. Ferroudji, "Random forest and filter bank common spatial patterns for EEG-based mi classification," in *2014 5th International Conference on Intelligent Systems, Modelling and Simulation*, 1 2014, pp. 235–238.
[12] C. Park, C. C. Took, and D. P. Mandic, "Augmented complex common spatial patterns for classification of noncircular EEG from motor imagery tasks," *IEEE Transactions on Neural Systems and Rehabilitation Engineering*, vol. 22, no. 1, pp. 1–10, 1 2014.
[13] Y. Kim, J. Ryu, K. K. Kim, C. C. Took, D. P. Mandic, and C. Park, "Motor imagery classification using mu and beta rhythms of EEG with strong uncorrelating transform based complex common spatial patterns," *Intell. Neuroscience*, vol. 2016, 2016.
[14] Y. LeCun, Y. Bengio, and G. Hinton, "Deep learning," *Nature*, vol. 521, no. 7553, pp. 436–444, 2015.
[15] S. Kumar, A. Sharma, K. Mamun, and T. Tsunoda, "A deep learning approach for motor imagery EEG signal classification," in *3rd Asia-Pacific World Congress on Computer Science and Engineering (APWC on CSE)*, 2016, pp. 34–39.
[16] P. Bashivan, I. Rish, M. Yeasin, and N. Codella, "Learning representations from EEG with deep recurrent-convolutional neural networks," *International Conference on Learning Representations (ICLR)*, 2016.
[17] Y. R. Tabar and U. Halici, "A novel deep learning approach for classification of EEG motor imagery signals," *Journal of Neural Engineering*, vol. 14, no. 1, p. 16003, 2017.
[18] Y. Shen, H. Lu, and J. Jia, "Classification of motor imagery EEG signals with deep learning models," in *Intelligence Science and Big Data Engineering: 7th International Conference, IScIDE 2017*. Springer International Publishing, 2017, pp. 181–190.
[19] R. T. Schirrmeister, J. T. Springenberg, L. D. J. Fiederer, M. Glasstetter, K. Eggensperger, M. Tangermann, F. Hutter, W. Burgard, and T. Ball, "Deep learning with convolutional neural networks for EEG decoding and visualization," *Human Brain Mapping*, vol. 38, no. 11, pp. 5391–5420, 2017.
[20] G. AL, A. LAN, G. L, H. JM, I. PCh, M. RG, M. JE, M. GB, P. C-K, and S. HE, "Physiobank, physiotoolkit, and physionet: Components of a new research resource for complex physiologic signals," *Circulation*, vol. 101, no. 23, pp. e215–e220, 2013, http://circ.ahajournals.org/cgi/content/full/101/23/e215.
[21] G. Schalk, D. McFarland, T. Hinterberger, N. Birbaumer, and J. Wolpaw, "BCI2000: A general-purpose brain-computer interface (BCI) system," *IEEE Transactions on Biomedical Engineering*, vol. 51, no. 6, pp. 1034–1043, 2004.

ISBN 978-90-827970-1-5 © EURASIP 2018